Comparison of Absorption-Emission Properties of New Azo Dyes and New Schiff Bases from Benzimidazole Derivative 1,3,4-Thiadiazole and Theoretical Calculation by DFT Method

Nesrin Şener[a, *] , **Sevil Özkınalı**[b] , **Mahmut Gür**[c] , **Merve Zurnacı**[d] , **İzzet Şener**[e] , **M. Serdar Çavuş**[f]

[a] Department of Chemistry, Faculty of Science, Kastamonu University, 37200, Kastamonu, Türkiye
[b] Department of Chemistry, Faculty of Science-Arts, Hitit University, Çorum, Türkiye
[c] Department of Forest Industrial Engineering, Faculty of Forestry, Kastamonu University, 37200, Kastamonu, Türkiye
[d] Institute of Science, Kastamonu University, 37200 Kastamonu, Türkiye
[e] Department of Food Engineering, Faculty of Engineering and Architecture, Kastamonu University, 37200, Kastamonu, Türkiye
[f] Department of Biomedical Engineering, Faculty of Engineering and Architecture, Kastamonu University, Kastamonu, Türkiye
*Corresponding Author: nsener@kastamonu.edu.tr

Abstract: After the synthesis of the new benzimidazole derivative 1,3,4-thiadiazole compound, a series of azo dyes from the reaction of this compound with various coupling components and a series of schiff bases were synthesized from the reaction with various aldehydes. The structures of the obtained compounds are characterized and interpreted with UV, FT-IR and ^{1}H-NMR. The fluorescence properties of the compounds were also investigated, and the absorption and emission properties of schiff base and azo dyes obtained from the same derivative were examined. As a result, it was observed that schiff bases obtained from benzimidazole derivative 1,3,4-thiadiazole compound had longer wavelength absorption-emission compared to azo dyes obtained from the same compound. Experimental data were supported by density functional theory (DFT) calculations. The ground state geometries, spectroscopic properties, FMO energies and related chemical reactivity parameters of the compounds were calculated using the B3LYP hybrid density functional combined with 6-311++G(2d,2p) basis set. At the same theory level, QTAIM and IRI analyzes were also performed and the data were used to determine the properties of tautomeric structures. The electronic properties of the compounds were studied and a detailed analysis was performed by comparing them with experimental data.

Keywords: Benzimidazole, Azo dyes, Schiff bases, Fluorescence, Absorption properties, DFT method

Öz: Yeni benzimidazol türevi 1,3,4-tiyadiazol bileşiğinin sentezinden sonra, bu bileşiğin çeşitli kenetleme bileşenleriyle reaksiyonundan bir dizi azo boya ve çeşitli aldehitlerle reaksiyonundan bir dizi schiff bazı sentezlenmiştir. Elde edilen bileşiklerin yapıları UV-Vis., FT-IR ve ^{1}H-NMR ile karakterize edilerek yorumlanmıştır. Bileşiklerin floresans özellikleri de araştırılmış, aynı türevden elde edilen schiff bazı ve azo boyaların absorpsiyon ve emisyon özellikleri de incelenmiştir. Sonuç olarak, benzimidazol türevi 1,3,4-tiyadiazol bileşiğinden elde edilen schiff bazlarının, aynı bileşikten elde edilen azo boyalara göre daha uzun dalga boyunda absorpsiyon-emisyona sahip olduğu gözlendi. Deneysel veriler, yoğunluk fonksiyonel teorisi (DFT) hesaplamaları ile desteklenmiştir. Bileşiklerin temel durum geometrileri, spektroskopik özellikleri, FMO enerjileri ve ilgili kimyasal reaktivite parametreleri, 6-311++G(2d,2p) temel seti ile birleştirilmiş B3LYP hibrit yoğunluk fonksiyoneli kullanılarak hesaplanmıştır. Aynı teori seviyesinde QTAIM ve IRI analizleri de yapılmış ve veriler tautomerik yapıların özelliklerini belirlemede kullanılmıştır. Bileşiklerin elektronik özellikleri incelenmiş ve deneysel verilerle karşılaştırılarak detaylı analiz yapılmıştır.

Anahtar Kelimeler: Benzimidazol, Azo boyalar, Schiff bazları, Floresans, Absorpsiyon özellikleri, DFT yöntemi

1. Introduction

Benzimidazoles are one of the most important *N*-containing organic compounds in a wide variety of natural products and pharmaceuticals [1,2]. Despite numerous attempts to develop new structural prototypes in the search for more effective antimicrobials, benzimidazoles continue to remain a versatile compound against microorganisms [3-10] and therefore, they are useful sub-structures for further molecular investigations. On the other hand, it has been shown in the literature that 1,3,4-thiadiazoles are also associated with pharmacological activities such as antimicrobial, antiviral, anesthetic and anticonvulsant [11-15]. Although not many, there are benzimidazole derivative 1,3,4-thiadiazole compounds in previous studies [16,17]. Similarly, antimicrobial activity studies of these compounds have been conducted.

Fluorescence property of molecules is a biologically important method due to its high sensitivity [18-21]. It is known that fluorescence spectroscopy has a wide application in both analytical and diagnostic studies as a very sensitive and informative method for the characterization of simple and complex molecules [22]. Therefore, it is very important to

study the absorption and emissions of organic molecules such as azo dyes and schiff bases, which are important in terms of their biological properties and have been studied by researchers. Fluorescent dyes are characterized by extraordinarily bright colors, as they not only absorb but also emit in the visibility [23, 24]. Fluorescent dyes are used for various applications, such as for a solid-state dye laser system [25], polymer treatment [26], optical fibres [27] and solid-state dye-labelled DNA [28] to detect volatile compounds in the vapor phase. It is possible to talk about similar fluorescent properties for Schiff bases. For example, while in a study a simple Schiff base (*Z*)-*N*-benzylidene naphthalen-1-amine (L) acts as an effective fluorescence sensor for Al^{+3} [29], in another study, a turn-on Schiff base for the Zinc ion is mentioned [30]. In a study, Guo synthesized some schiff-base macromolecular ligand by copolymerizing schff-base monomer, methyl methacrylate and ethyl acrylate. After preparation of the polymeric materials based on terbium complex with this macromolecular ligand, the fluorescence properties of the terbium-complex polymer were investigated experimentally [31].

In present study, in the first step, we obtained 1,3,4-thiadiazole derivative from the reaction of benzimidazole-5-carboxylic acid and thiosemicarbazide. In the next step, we synthesized five different azo dyes and five different schiff bases from this 1,3,4-thiadiazole derivative. These compounds obtained after the experimental stage were characterized by spectroscopic methods such as ^{1}H-NMR and FT-IR. Then, the absorption and emission measurements of these synthesis compounds were examined and discussed. In addition, DFT calculations were performed for a theoretical analysis of experimental results. Electronic parameters such as highest occupied molecular orbital (HOMO), lowest unoccupied molecular orbital (LUMO) energies, electronegativity (χ), chemical hardness (η), and polarizability (α), electrophilic index (ω), nucleophilic index (ε), electrodonating power (ω^-) were calculated at the B3LYP/6-311++G(2d,2p) level of theory. FT-IR, UV-Vis and ^{1}H-NMR spectra of the compounds were obtained using the same method and basis set. The relationship between tautomeric transitions and electronic properties of compounds was investigated theoretically.

2. Material and Method

Benzophenone-4,4'-dicarboxylic acid was purchased from TCI chemicals whereas phosphorous oxychloride (99%) was from Merck. Thiosemicarbazide was provided from Sigma-Aldrich, ethanol solvent was bought from Tekkim Company. Melting points were taken with Stuart SMP10 apparatus. UV-Vis. absorption spectra were recorded with Shimadzu UV Mini-1240 UV-Vis. spectrophotometer by using cyclohexanone, DMF, 1,4-dioxane and DMSO (by Merck) as solvent. FT-IR spectra were taken in the region 400-4000 cm^{-1} on Alpha FTIR spectrometer Bruker. The ^{1}H-NMR spectra were recorded on Bruker AVANCE III 400 MHz NMR spectrophotometer at room temperature in dimethyl sulfoxide-d$_6$ (DMSO-d$_6$). The photoluminescence (PL) spectra were recorded in a 1 cm path length quartz cell using a Horiba FluoroMax-4 fluorescence spectrometer.

Synthesis of compound 1

Benzimidazole carboxylic acid compound (n mol), thiosemicarbazide (n mol) and POCl$_3$ (3 mol) were placed in a 100 mL flask and refluxed for 3 hours at 90 °C, cooled, 50 mL of cold water was added and mixed, then filtered. The filtrate was neutralized with 25% aqueous NH$_3$. The precipitate formed was separated by filtration. It was washed with water, dried and purified (compound 1). The yield was calculated by weighing the dried sample. The melting point was checked. Final product; FT-IR, ^{1}H-NMR. Yield: 72% m.p 295 °C. IR ν (cm^{-1}) = 3250 (-NH$_2$), 3113 (-NH), 3021 (C-H$_{arom.}$), 1643 (-CH=N-), 1622 (-C=C-), 708 (-C-S-C-).^{1}H-NMR (d$_6$-DMSO, ppm): δ= 7,35 (s, 2H, -NH$_2$), 7,90-8,66 (aromatic C-H), 8,53 (s,-NH); The synthesis reaction pattern is shown in Figure 1.
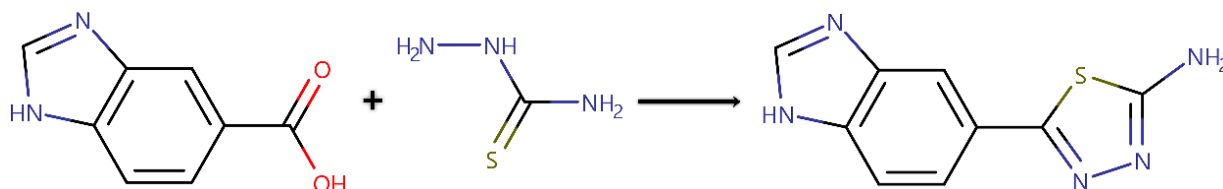

Figure 1. Synthesis reaction of compound 1.

General Synthesis Method of Compound 2(a-e)

Obtained benzimidazole derivative 1,3,4-thiadiazole compound (Compound 1) (n mol) is dissolved in HCl (3 mL) and acetic acid (6 mL), and added NaNO$_2$, which is dissolved in sulfuric acid at the minimum rate, mixed in the range of 0-5 ºC to prepare the diazonium salt. After two hours, it was stirred at 0-5 °C for 2 hours with the addition of various coupling compounds (n mol) in basic medium. As a result of the coupling reaction, five different azo dyes were synthesized. The synthesis reaction pattern is shown in Figure 2.

(*E*)-3-((5-(1*H*-benzo[d]imidazol-5-yl)-1,3,4-thiadiazol-2-yl)diazenyl)-4-hydroxyquinolin-2(3H)-one   (Compound 2a)

Yield: 62% m.p 340 °C. IR ν (cm⁻¹) = 3256 (-OH), 3154 (-NH), 3092 (C-H$_{arom.}$), 1658 (C=O), 1630 (C=C), 1606 (-C=N-), 1564-1469 (N=N), 723 (-C-S-C-).¹H-NMR (DMSO-d$_6$, ppm): δ= 5.71 (1H, s, benzimidazole -NH), 7.07-7,83 (8H, aromatic C-H),), 11.17 ve 11.28 (2H, s, -OH).

(*E*)-2-((5-(1*H*-benzo[d]imidazol-5-yl)-1,3,4-thiadiazol-2-yl)diazenyl)naphthalen-1-ol (Compound 2b)

Yield: 71% m.p 260 °C. IR ν (cm⁻¹) = 3283 (-OH), 3167 (-NH), 3092 (C-H$_{arom.}$), 1620 (-C=C-), 1548-1409 (N=N), 1101 (C-O), 691 (-C-S-C-).¹H-NMR (DMSO-d$_6$, ppm): δ=7.33-8.49 (10H, aromatic C-H), 10.07 (1H, s, -OH).

(*E*)-3-((5-(1*H*-benzo[d]imidazol-5-yl)-1,3,4-thiadiazol-2-yl)diazenyl)-4-hydroxy-2H-chromen-2-one   (Compound 2c)

Yield: 61% m.p 290 °C. IR ν (cm⁻¹) = 3342 (-OH), 3209 (-NH), 3093 (C-H$_{arom}$), 1682 (C=O), 1615 (-C=C-), 1599 (-C=N-), 1516-1448 (N=N), 1051 (C-O), 734 (C-S-C).   ¹H-NMR (400 MHz, DMSO-d$_6$) δ (ppm): 5.60 (1H, s, benzimidazole -NH), 7.32-8,00 (8H, aromatic C-H), 8.42 (1H, s, -OH).

(*E*)-4-((5-(1*H*-benzo[d]imidazol-5-yl)-1,3,4-thiadiazol-2-yl)diazenyl)-3-methyl-1H-pyrazol-5-ol (Compound 2d)

Yield: 67% m.p 315 °C. IR ν (cm⁻¹) = 3271 (-OH), 3115 (-NH), 3094 (C-H$_{arom}$), 2988 (C-H$_{aliphatic}$), 1614 (-C=C-), 1545-1449 (N=N), 1036 (C-O), 769 (C-S-C). ¹H-NMR (400 MHz, DMSO-d$_6$) δ (ppm): 2.50 (3H, s, -CH₃), 4.83 (1H, s, benzimidazole -NH), 7.39-8,12 (4H, aromatic C-H), 8.91 (1H, s, pyrazole -NH).

(*E*)-4-((5-(1*H*-benzo[d]imidazol-5-yl)-1,3,4-thiadiazol-2-yl)diazenyl)-3-methyl-1-phenyl-1H-pyrazol-5-ol (Compound 2e)

Yield: 68% m.p 310 °C. IR ν (cm⁻¹) = 3272 (-OH), 3112 (-NH), 3092 (C-H$_{arom}$), 2913 (C-H$_{aliphatic}$), 1613 (C=C), 1546-1449 (N=N), 689 (C-S-C). ¹H-NMR (400 MHz, CDCl₃) δ (ppm): 2.51 (3H, s, -CH₃), 5.93 (1H, s, benzimidazole -NH), 7.37-8,05 (9H, aromatic C-H), 8.87 (1H, -OH).
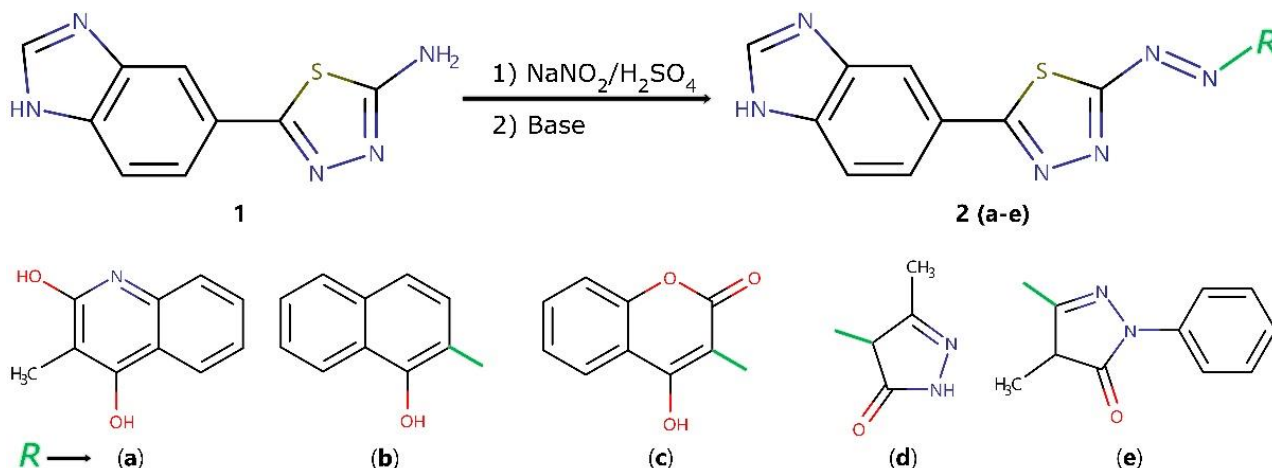

Figure 2. Synthesis reaction of compound 2(a-e).

General Synthesis Method of Compound 3(a-e)

The obtained compound 1 was reacted with various aldehydes in ethanol (50 mL) at a ratio of 1:1 in reflux for 24 hours, and the precipitates formed in the reaction chamber were filtered and crystallized. Afterwards, structural analysis of these five different schiff base derivatives was performed with different spectroscopic methods. The synthesis reaction pattern is shown in Figure 3.

(*E*)-5-(1*H*-benzo[d]imidazol-5-yl)-*N*-(4-methoxybenzylidene)-1,3,4-thiadiazol-2-amine (Compound 3a)

Yield: 74% m.p 285 °C. IR ν (cm⁻¹) = 3121 (-NH), 3039 (C-H$_{arom}$), 2918-2824 (C-H$_{aliphatic}$), 1665 (N=CH), 1622 (C=C), 1099 (C-O), 730 (C-S-C). ¹H-NMR (400 MHz, DMSO-d$_6$) δ (ppm): 3.43 (3H, s, -OCH₃), 7.31 (1H,s, -NH), 7.63-8,46 (8H, aromatic C-H), 8.53 (1H, s,-N=CH).

(*E*)-4-(((5-(1*H*-benzo[d]imidazol-5-yl)-1,3,4-thiadiazol-2-yl)imino)methyl)phenol (Compound 3b)

Yield: 75% m.p 280 °C. IR ν (cm⁻¹) = 3351 (-OH), 3186 (-NH), 3048 (C-H$_{arom}$), 2912 (C-H$_{aliphatic}$), 1652 (N=CH), 1624 (C=C), 1594 (C=N), 1108 (C-O), 730 (C-S-C). ¹H-NMR (400 MHz, DMSO-d$_6$) δ (ppm): 6.96 (1H, s, -NH), 7.30-8.47 (8H, aromatic C-H), 8.91 (1H, s, N=CH), 10.63 (1H, s, -OH).

(*E*)-5-(1*H*-benzo[d]imidazol-5-yl)-*N*-(4-chlorobenzylidene)-1,3,4-thiadiazol-2-amine (Compound 3c)

Yield: 71% m.p 280 °C. IR ν (cm^{-1}) = 3122 (-NH), 3065 (C-H$_{arom}$), 2921 (C-H$_{aliphatic}$), 1653 (-N=CH), 1622 (C=C), 738 (C-S-C). ^{1}H-NMR (400 MHz, DMSO-d$_6$) δ (ppm): 7.33 (1H, s, -NH), 7.72-8,48 (8H, aromatic C-H), 8.53 (1H, s, -N=CH).

(*E*)-5-(1*H*-benzo[d]imidazol-5-yl)-*N*-(4-nitrobenzylidene)-1,3,4-thiadiazol-2-amine (Compound 3d)

Yield: 74% m.p 220 °C. IR ν (cm^{-1}) = 3113 (-NH), 3083 (C-H$_{arom}$), 2965 (C-H$_{aliphatic}$), 1648 (N=CH), 1624 (C=C), 1557 (-NO$_2$), 729 (C-S-C). ^{1}H-NMR (400 MHz, DMSO-d$_6$) δ (ppm): 7.32 (1H, s, -NH), 7.62-8,06 (8H, aromatic C-H), 10.17 (1H, s, N=CH).

(*E*)-5-(1*H*-benzo[d]imidazol-5-yl)-*N*-(4-fluorobenzylidene)-1,3,4-thiadiazol-2-amine (Compound 3e)

Yield: 73% m.p 275 °C. IR ν (cm^{-1}) = 3139 (-NH), 3096 (C-H$_{arom}$), 2907 (C-H$_{aliphatic}$), 1652 (N=CH), 1623 (C=C), 732 (C-S-C). ^{1}H-NMR (400 MHz, DMSO-d$_6$) δ (ppm): 7.34 (1H, s, NH), 7.63-8,46 (8H, aromatic C-H), 8.53 (1H, s, -N=CH).
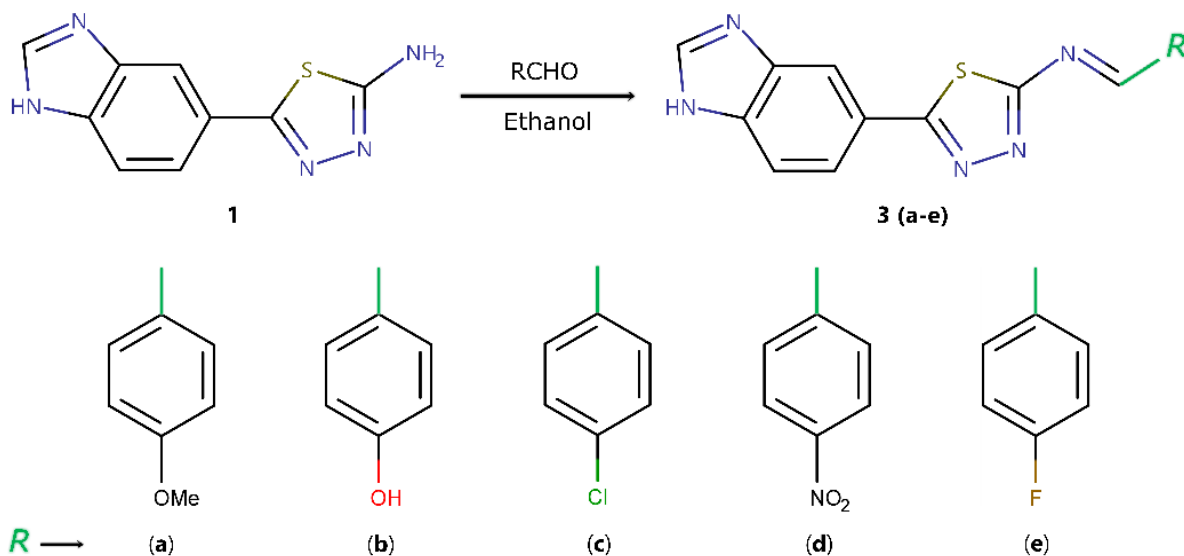

Figure 3. Synthesis reaction of compound 3(a-e).

Absorption and Emission Study

The absorption and emission studies were determined using UV-Vis. (Shimadzu) and fluorescence spectroscopy (Horiba, Fluoromax-3). The absorption and fluorescence emission spectra were studied in DMF and DMSO of all the compounds (concentration of 1×10^{-5} M). The maximum absorption, maximum emission wavelength and Stokes shift are listed in Table 3 for all the compounds.

Computational procedure

First, the compounds were scanned dihedrally using the B3LYP/6-31G theoretical approach to determine the minimum energy conformations (Figure 4). The minimum energy conformations obtained from the dihedral scan were used as input data for all other calculations. All DFT [32, 33] calculations were performed using Gaussian 09 software [34], using B3LYP/6-311++G(2d,2p) level of theory. The optimized state geometries correspond to the global minimum energy points on the potential energy surface, so no imaginary frequencies were observed in the IR calculations performed in the gas phase.
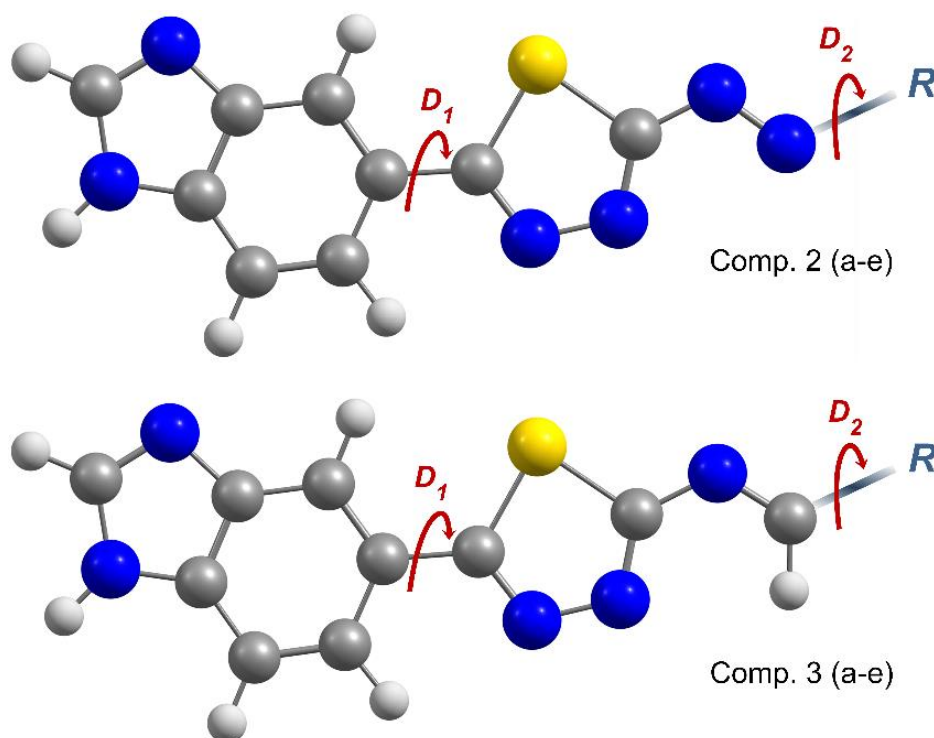
Figure 4. Dihedral scanning of the compounds 2(a-e) and 3(a-e) by 360 steps with a 20-degree rotations D_1 and D_2.

In parallel with the acquisition of experimental NMR data in dimethyl sulfoxide (DMSO) solvent, DFT/^{1}H-NMR calculations were also performed in the DMSO phase using Gauge-independent atomic orbital (GIAO) method, and conductor-like polarizable continuum model (CPCM) was used for solution–solvent interaction in these processes. Relative chemical shift values were calculated by subtracting the absolute chemical shielding of tetramethylsilane (TMS) performed at the B3LYP/6-311++G(2d,2p) level (31,8149 ppm for ^{1}H-NMR).

The IR calculations were performed in the gas phase and the electronic parameters of the compounds were also obtained from the gas phase calculations. Global chemical reactivity parameters such as HOMO-LOMO energy gap (E_g), chemical hardness (η), electronegativity (χ), electrophilic index (ω), nucleophilic index (ε), and electrodonating power indices (ω^-) were calculated using frontier molecular orbital (FMO) energy eigenvalues obtained from IR calculations.

The electron density on the ring critical points (RCPs) and bond critical points (BCPs) of the compounds was determined using the QTAIM approach [35, 36]. Also, using Multiwfn software [37], interaction region indicator (IRI) calculations were performed to visualize intramolecular interactions.

3. Result and Discussion

The reaction procedures of the synthesized compounds were carried out as shown in Figure 1 and Figure 2. Based on the benzophenone-4,4-dicarboxylic acid compound, five new azo dyes and five new Schiff bases were obtained with 61-75% efficiency. Spectroscopic methods such as ^{1}H-NMR and FT-IR were used to characterize the structures of the synthesized compounds.

When we look at the FT-IR spectrum results (in Table 1), we see –OH stretching vibrations of the compounds in the range of 3351-3271 cm^{-1}. We see the bands resulting from –NH stretching vibrations in the structures in the range of 3209-3113 cm^{-1}. While we observe aromatic –CH stretching vibrations in the molecules in the range of 3094-3039 cm^{-1}, we observe aliphatic –CH stretching vibrations in the range of 2965-2824 cm^{-1}. The C=O stretching vibration bands observed for compounds 2a and 2c are 1658 and 1682 cm^{-1}, respectively. N=CH stretching vibrations of compounds 3(a-e) are observed in the range of 1665-1648 cm^{-1}. In generally, the C=C stretching vibrations of the compounds are observed in the range of 1630-1613 cm^{-1}, while the bands of the C=N stretching vibrations are observed in the range of 1606-1599 cm^{-1}. The stretching and bending vibrations of azo bridges with compound 2(a-e) are observed in the range of 1564-1516 cm^{-1} and 1469-1409 cm^{-1}, respectively. The stretching vibrations of the C–O bonds in the molecular structures were observed in the range of 1108-1036 cm^{-1}. The bands of stretching vibrations of C–S–C bonds in all compounds obtained were seen in the range of 732-689 cm^{-1}.

Table 1. Experimental and theoretical FT-IR spectrum results of the compounds (cm^{-1}). (Scaling factors: 0.901 for –OH, 0.861 for –NH, 0.963 for C–H (Ar.), 0.948 for C–H (Alip.), 0.937 for C-S-C)

	Com.	υ(-OH)	υ(-NH)	υC-H (Ar.)	υC-H (Alip.)	υC=O	υN=CH	υC=N thiadiazol	υ(NO2)	υ(N=N)	υ(C-O)	υC-S-C
Experimental	2a	3256	3154	3092	-	1658	-	1606	-	1564,1469	-	723
	2b	3283	3167	3092	-	-	-	-	-	1548, 1409	1101	691
	2c	3342	3209	3093	-	1682	-	1599	-	1516, 1448	1051	734
	2d	3271	3115	3094	2988	-	-	-	-	1545, 1449	1036	769
	2e	3272	3212	3092	2913	-	-	-	-	1546, 1449	-	689
	3a	-	3121	3039	2918, 2824	-	1665	-	-	-	1099	730
	3b	3351	3186	3048	2912	-	1652	-	-	-	1108	730
	3c	-	3122	3065	2921	-	1653	-	-	-	-	738
	3d	-	3113	3083	2965	-	1648	-	1557, 1448	-	-	729
	3e	-	3139	3096	2907	-	1652	-	-	-	-	732
Calculated	2a-T	3301	3152	3100-3058	-	1766	-	1435, 1383	-	1570	-	726
	2b	3245	3153	3099-3064	-	-	-	1424, 1380	-	1481	1221	725
	2c	3131	3153	3099-3067	-	1712	-	1431, 1381	-	1511	1124	726
	2d-T	3333	3163, 3155	3099-3066	2968-2883	-	-	1432, 1390	-	1491	1112	726
	2e-T	3300	3158	3099-3066	2969-2883	-	-	1430, 1382	-	1487	1091	729
	3a	-	3153	3098-3056	2910	-	1624	1448, 1425	-	-	1052	729
	3b	3449	3155	3098-3042	2912	-	1629	1450, 1425	-	-	1290	735
	3c	-	3154	3098-3059	2915	-	1649	1452, 1421	-	-	-	720
	3d	-	3154	3099-3067	2921	-	1652	1450, 1398	1562, 1363	-	-	718
	3e	-	3153	3098-3061	2913	-	1654	1455, 1422	-	-	-	732

2(a-e)-T: Expresses the values of the tautomeric form of the compounds.

When we look at the ^{1}H-NMR spectrum results (in Table 2), we see the peaks of aliphatic protons in the range of 2.50-3.43 ppm, and the aromatic peaks in the range of 7.07-8.49 ppm. While we see the peaks of –*N*H protons in the range of 5.71-8.91 ppm, we see the peaks of –*O*H protons in the range of 8.42-11.28 ppm. We observe the peaks of *N=C*H protons in Schiff base compounds in the range of 8.53-10.17 ppm. In addition, all the peaks of the compounds are compatible with the integration rates.

Table 2. Experimental and theoretical ^{1}H-NMR spectrum results of the compounds (ppm).

	Comp.	*Aliphatic*-H	*Aromatic*-H	*N*-H	*O*-H	*N=C*-H
Experimental	2a	-	7.83-7.07	5.71	11.17, 11.28	-
	2b	-	8.49-7.33	-	10.07	-
	2c	-	8.00-7.32	5.60	8.42	-
	2d	2.50 (3H, s, -CH$_3$)	8.12-7.39	8.91	-	-
	2e	2.51(3H, s, -CH$_3$)	8.05-7.37	5.93	8.87	-
	3a	3.43 (3H, s, -OCH$_3$)	8.46-7.63	-	-	8.53
	3b	-	8.47-7.30	6.96	10.63	8.91
	3c	-	8.48-7.72	7.33	-	8.53
	3d	-	8.06-7.62	7.32	-	10.17
	3e	-	8.46-7.63	7.34	-	8.53
Calculated	2a	-	8.94-7.85	9.50	15.06, 9.11	-
	2b	-	8.97-7.81	9.47	9.91	-
	2c	-	8.93-7.98	9.48	10.76	-
	2d	2.33-2.07 (-CH$_3$)	8.91-5.12	9.50, 8.26	-	-
	2e-T	2.70-2.51 (-CH$_3$)	8.89-7.87	9.46	7.92	-
	3a	4.25-4.02 (-OCH$_3$)	8.85-7.42	9.43	-	9.31
	3b	-	8.81-7.28	9.43	5.55	9.30
	3c	-	8.83-7.94	9.44	-	9.41
	3d	-	9.01-7.99	9.45	-	9.61
	3e	-	8.86-7.65	9.44	-	9.40

The maximum absorption, maximum emission wavelength and Stokes shift are listed in Table 3 for all the compounds. Absorption and emission properties of the compounds changed with solvents. Absorption and emission bands were observed at between 264-321 nm and 324-339 nm, respectively. When comparing the absorption and emission bands of all compounds; it was observed that the wavelengths of compounds in DMSO were higher than DMF. The compound with the highest maximum Stokes shift in DMSO was determined as 2c. The calculated UV absorption rates are given in Figure 5 and it was observed to be in agreement with the experimental results.

The structure of the compounds has been to cause a change in fluorescence emission properties. The maximum fluorescence emission wavelength was determined as the compounds bearing -OH, C=O and –O– (2a, 2c and 3b). At the same time, the Stokes shift of the compounds including –OH, C=O and –O– (in aromatic ring) bond was wider when compared to the other compounds. These compounds contribute to the delocalization due to the electron-donating and activator properties of the –OH, C=O and –O– groups.

Table 3. Absorption-emission properties of the compounds in different solvents (nm)

| Comp.	Solvent	Absorbance (nm) λ_{max}	Emission (nm) λ_{max}	Stokes' shift (nm)
2a	DMF	321	439	118
	DMSO	271,281,321,338	439	119
2b	DMF	316	424	108
	DMSO	317	435	118
2c	DMF	308	434	126
	DMSO	264,282,308,320	439	131
2d	DMF	317	427	110
	DMSO	319	436	117
2e	DMF	319	432	113
	DMSO	318	437	119
3a	DMF	314	430	116
	DMSO	316	435	119
3b	DMF	316	423	107
	DMSO	319	438	119
3c	DMF	307	430	123
	DMSO	311	437	126
3d	DMF	315	428	113
	DMSO	318	436	118
3e	DMF	320	424	104
	DMSO	321	435	114
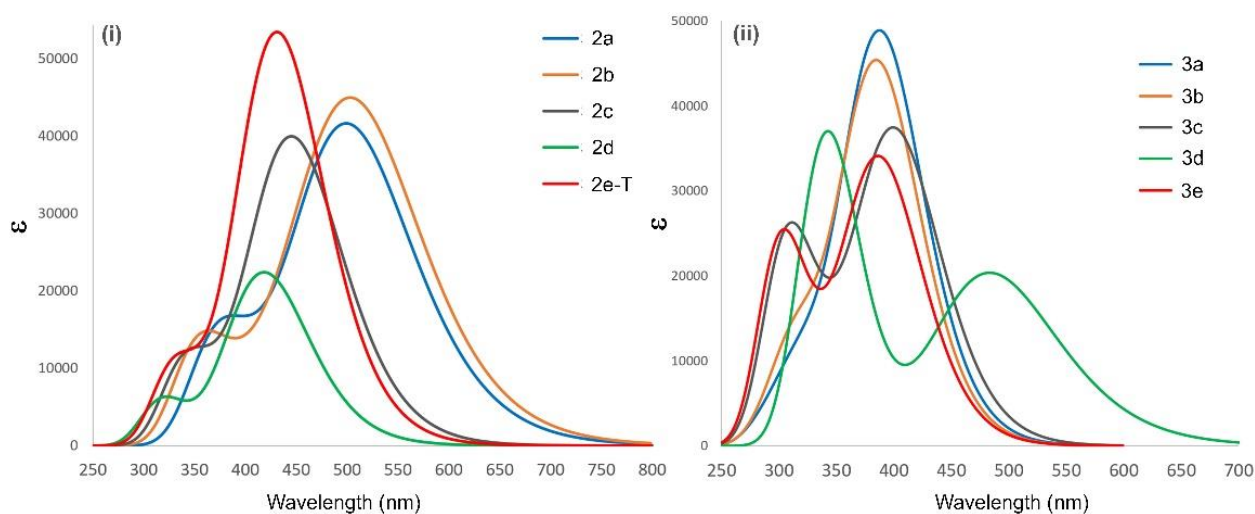
Figure 5. Calculated UV-Vis. absorption peaks of the compounds.

Computational results

Although global chemical reactivity parameters (GCRPs) such as HOMO-LUMO energy gap, electronegativity, chemical hardness, etc. [38, 39], give clues about some basic properties and behaviors of molecular structures, these calculated properties of single molecules (independent of environmental effects, without atomic or molecular pollution) are can not meet the variable electronic properties of molecular structures. In other words, GCRPs can be used to predict how a compound will propensity for any given reaction, but the dependence of a reaction on macro variables such as temperature as well as electronic variables such as the interaction of molecules with the environment and intramolecular interactions makes it difficult to interpret GCRPs calculated on a single molecule structure. However, the ability of the reactions to repeat themselves in experiments with approximately the same results reveals that the relevant reaction is driven by some dominant variables. Thus, it can be said that one or more of the GCRPs may overlap with experimental data in some cases. Starting from this point, some GCRPs of first group 2(a-e) and second group 3(a-e) compounds were calculated and possible reaction characteristics of these compounds were determined (The all values of the calculated GCRPs are given in the Supplementary Table S1).

Calculations for the tautomers of the compounds, which are compounds 2a, 2d, 2e and 2a-T, 2d-T, 2e-T, did not reveal sufficient results to predict a correlation between the total electronic energy and the tautomeric conformational preference. In other words, the data are not sufficient to make the assumption that a lower energy tautomer can be observed more frequently in experiments. However, the HOMO-LUMO energy gap E_g was calculated to be lower in tautomers (2a, 2d, and 2e-T) with intramolecular interacting hydrogens (Figure 5-c). At this point, it can be said that these tautomers have higher chemical reactivity and lower kinetic stability. The results reveal that it is difficult to say that HOMO or LUMO energies are directly related to the characteristics of tautomer structures (see Figure 5-b).
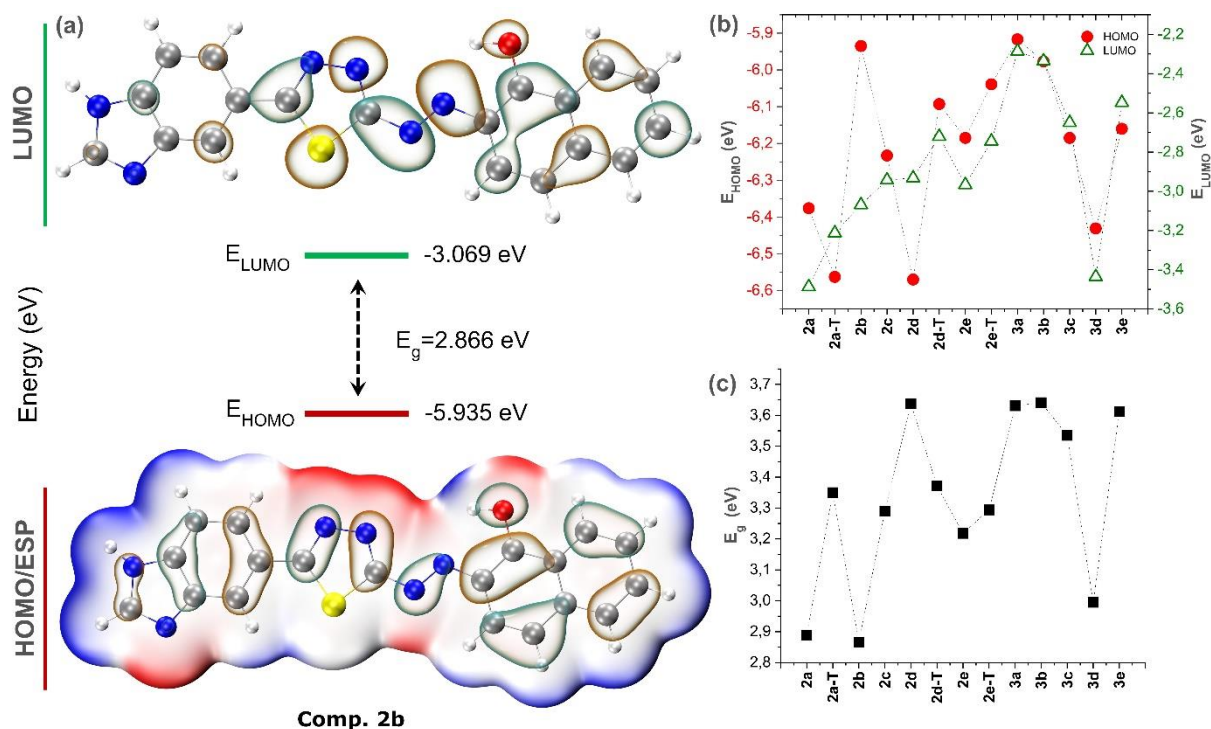

Figure 5. HOMO/ESP and LUMO surfaces (a), HOMO and LUMO energy eigenvalues (b), and HOMO-LUMO energy gap (c) of the compound 2b.

The electronegativity, electrophilic index, and electrodonating power parameters related to the electron affinities of the compounds (Figure 6), reveal that the second group compounds may show higher nucleophilic behavior than the first group compounds, except NO_2 substituted 3d. In addition, both electrophilic indexes and electrodonating power values of tautomers structures 2a-T, 2d-T, and 2e-T were calculated. These results strengthen the conclusion that the synthesis mechanism of the compounds leads them to become nucleophilic. At this point, it should be noted that since the conformations of the tautomers structures selected for the calculations directly affect the calculation results, precise interpretations of the present results cannot be made easily.
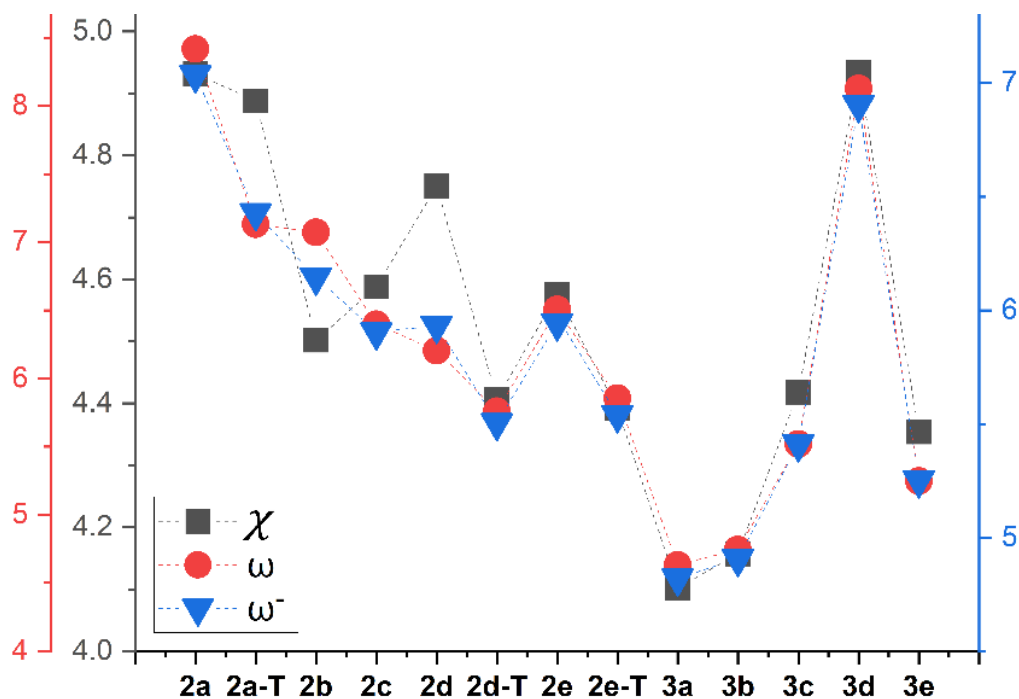
Figure 6. Electronegativity, χ (eV), electrophilic index, ω (eV), and electrodonating power, ω⁻ (eV) values of the compounds.

IRI and QTAIM calculations were performed to analyze intramolecular interactions and electron charge distributions. Intramolecular interactions for tautomers 2a and 2a-T and IRI surface maps of the intensities of these interactions are in Figure 7, and the calculated charge densities in BCP and RCP are given in Table 4 (see Supplementary Figure S1 for IRI maps of the compounds). The variation of the electron density of the structure to which the hydrogen atom causing the tautomer is attached is quite evident for both visual (for IRI) and calculated values (for QTAIM) on R4 and B(3-7). In addition, although the substituted groups and the structures attached to these groups changed, it was observed that the electron density in the RCPs of these rings changed less than in other RCPs due to the high pi conjugation on the phenyl rings.
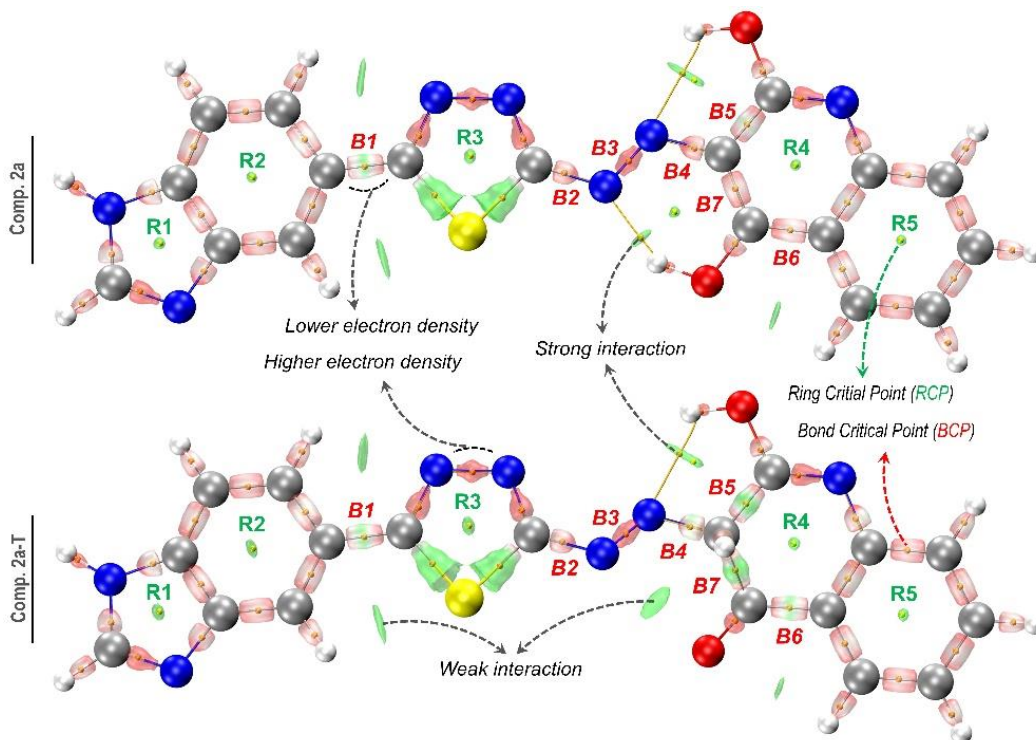

Figure 7. IRI maps and QTAIM data of compounds 2a and 2a-T.

Table 4. Calculated electron charge density of compounds in selected BCPs and RCPs, (e/bohr^3)

	2a	2a-T	2b	2c	2d	2d-T	2e	2e-T	3a	3b	3c	3d	3e
R1	0.057196	0.057203	0.057161	0.057166	0.057189	0.057152	0.057192	0.057162	0.057126	0.057130	0.057150	0.057175	0.057147
R2	0.022633	0.022637	0.022637	0.022638	0.022639	0.022639	0.022639	0.022635	0.022642	0.022643	0.022641	0.022638	0.022642
R3	0.046583	0.047008	0.046548	0.046706	0.046932	0.046495	0.046936	0.046414	0.045980	0.046004	0.046122	0.046253	0.046100
R4	0.023393	0.021648	0.021418	0.021345	-	-	-	-	0.022942	0.022966	0.023262	0.023527	0.023196
R5	0.022400	0.022927	0.022541	0.023354		-		-	-	-	-	-	-
B1	0.273435	0.273461	0.272865	0.272714	0.272943	0.272393	0.272995	0.272623	0.271692	0.271734	0.272012	0.272599	0.271924
B2	0.317860	0.311277	0.319728	0.317411	0.309458	0.318206	0.309446	0.318756	0.323116	0.322729	0.321319	0.320467	0.321418
B3	0.427902	0.466308	0.441828	0.446186	0.466886	0.438184	0.467047	0.422168	0.377345	0.377724	0.379438	0.380238	0.379400
B4	0.325761	0.280001	0.316802	0.317229	0.274831	0.328973	0.273856	0.334485	0.282858	0.282541	0.280166	0.278642	0.280328
B5	0.288311	0.253603	0.315143	0.316698		-		-	-	-	-	-	-
B6	0.302270	0.273534	0.331881	0.264106		-		-	-	-	-	-	-
B7	0.308856	0.230466	0.293874	0.274999		-		-	-	-	-	-	-

4. Conclusions

In this study, five different benzimidazole derivatives azo dyes and five different benzothiazole derivatives Schiff base derivatives were synthesized. Some GCRPs of the compounds were calculated and possible reaction properties were determined. No linear relationship was observed between the tautomeric transitions and the electronic energy of the compounds. However, E_g was calculated lower for tautomers with intermolecular interacting hydrogens. A moderately high correlation was observed between the electronegativity and electrophilic indices of the compounds, indicating that especially HOMO energy values can be used to directly predict the reactivity of a compound. IRI surfaces overlap with QTAIM data, highlighting the usefulness of IRI calculations, which are easier than QTAIM calculations. In addition, IRI calculations reveal intense intramolecular interactions in compounds. Intramolecular interactions reduce the freedom of compounds to dihedral rotations and this may be one of the reasons why the emission peaks come at low wavelengths.

Competing Interest / Conflict of Interest

The authors declare that they have no competing interests.

Author Contribution

We declare that all Authors equally contribute.

5. References

[1] Anthony, R. P., Rodrigo, V.D., Louis, S.K., John, C.D., & Leroy, B.T. (1998). Design, synthesis, and antiviral evaluations of 1-(Substitutedbenzyl)-2-substituted-5,6 dichlorobenzimidazoles as nonnucleoside analogues of 2,5,6-Trichloro-1-(b-D ribofuranosyl) benzimidazole. Journal of Medicinal Chemistry. 41(8), 1252-1262.

[2] Bansal, Y., & Silakari, O. (2012). The therapeutic journey of benzimidazoles: a review. Bioorganic & Medicinal Chemistry. 20(21), 6208-6236.

[3] Bishop, B.C., Chelton, E.T.J., & Jones, A.S. (1964). Biochemical Pharmacology. 13(5), 751-754.

[4] Habib, N.S., Soliman, R., Ashoura, F.A., & El-Taiebi, M. (1997). Synthesis and antimicrobial testing of novel oxadiazolylbenzimidazole derivatives. Die Pharmazie, 52(10), 746-749.

[5] Tuncbilek, M., Goker, H., Ertan, R., Eryigit, R., Kendi, E., & Altanlar, E. (1997). Synthesis and antimicrobial activity of some new anilino benzimidazoles. Archiv der Pharmazie, 330(12), 372-376.

[6] Göker, H., Tunçbilek, M., Süzen, S., Kus, C., & Altanlar, N. (2001). Synthesis and Antimicrobial Activity of Some New 2-Phenyl-N-substituted Carboxamido-1H-benzimidazole Derivatives. Archiv der Pharmazie: An International Journal Pharmaceutical and Medicinal Chemistry, 334(5), 148-152.

[7] Göker, H., Kuş, C., Boykin, D. W., Yildiz, S., & Altanlar, N. (2002). Synthesis of some new 2-substituted-phenyl-1H-benzimidazole-5-carbonitriles and their potent activity against Candida species. Bioorganic & medicinal chemistry, 10(8), 2589-2596.

[8] Pawar, N. S., Dalal, D. S., Shimpi, S. R., & Mahulikar, P. P. (2004). Studies of antimicrobial activity of N-alkyl and N-acyl 2-(4-thiazolyl)-1H-benzimidazoles. European journal of pharmaceutical sciences, 21(2-3), 115-118.

[9] Mohamed, B. G., Hussein, M. A., Abdel-Alim, A. A. M., & Hashem, M. (2006). Synthesis and antimicrobial activity of some new 1-alkyl-2-alkylthio-1, 2, 4-triazolobenzimidazole derivatives. Archives of pharmacal research, 29, 26-33.

[10] Vaidya, S. D., Kumar, B. V. S., Kumar, R. V., Bhise, U. N., & Mashelkar, U. C. (2007). Synthesis, anti-bacterial, anti-asthmatic and anti-diabetic activities of novel N-substituted-2-(benzo [d] isoxazol-3-ylmethyl)-1H-benzimidazoles. Journal of heterocyclic chemistry, 44(3), 685-691.

[11] Hogale, M. B., Uthale, A. C., & Nikam, B. P. (1991). hydrazidophenothiazines (IV). These intermediate inhibitory concentration (MIC) in mg/ml. The MIC. Indian Journal of Chemistry: Organic including medicinal. Section B, 30, 717-720.

[12] Srivastava, S. K., Srivastava, S., & Srivastava, S. D. (2002). Synthesis of new 1, 2, 4-triazolo-thiadiazoles and its 2-oxoazetidines as antimicrobial, anticonvulsant and antiinflammatory agents. Indian Journal of Chemistry. 41B, 2357-2363.

[13] Desai, K. G., & Desai, K. R. (2006). Green route for the heterocyclization of 2-mercaptobenzimidazole into β-lactum segment derivatives containing–CONH–bridge with benzimidazole: Screening in vitro antimicrobial activity with various microorganisms. Bioorganic and medicinal chemistry, 14(24), 8271-8279.

[14] Furniss, B.S., Hannaford, A.J., Smith, P.W.G., & Tatchell, A.R. (Eds.) (1998). Vogel's Text Book of Practical Organic Chemistry. ELBS Longman, England.

[15] Gür, M., Yerlikaya, S., Şener, N., Özkınalı, S., Baloglu, M. C., Gökçe, H., ... & Şener, İ. (2020). Antiproliferative-antimicrobial properties and structural analysis of newly synthesized Schiff bases derived from some 1, 3, 4-thiadiazole compounds. Journal of Molecular Structure, 1219, 128570.

[16] Ashour, F. A., Habib, N. S., El Taibbi, M., El Dine, S., & El Dine, A. S. (1990). Synthesis of 1, 3, 4-thiadiazoles, imidazo [2, 1-b] 1, 3, 4-thiadiazoles and thiadiazolo [3, 2-a] pyrimidines derived from benzimidazole as potential antimicrobial agents. Farmaco (Societa Chimica Italiana: 1989), 45(12), 1341-1349.

[17] Habib, N. S., Soliman, R., Ashour, F. A., & El-Taiebi, M. (1997). Synthesis and antimicrobial testing of 4H-1, 2, 4-triazole, 1, 2, 4-triazolo [3, 4-b][1, 3, 4] thiadiazole and 1, 2, 4-triazolo [3, 4-b][1, 3, 4] thiadiazine derivatives of 1H-benzimidazole. Die Pharmazie, 52(11), 844.

[18] Valeur, B., & Brochon, J. C. (Eds.). (2012). New trends in fluorescence spectroscopy: applications to chemical and life sciences (Vol. 1). Springer Science & Business Media.

[19] Strianese, M., Staiano, M., Ruggiero, G., Labella, T., Pellecchia, C., & D'Auria, S. (2012). Fluorescence-based biosensors. Spectroscopic methods of analysis: methods and protocols, 193-216.

[20] Goldys, E. M. (2009). Fluorescence applications in biotechnology and life sciences. John Wiley & Sons.

[21] Kraayenhof, R., Visser, A. J., & Gerritsen, H. C. (Eds.). (2012). Fluorescence spectroscopy, imaging and probes: new tools in chemical, physical and life sciences (Vol. 2). Springer Science & Business Media.

[22] Kalauzi, A., Mutavdžić, D., Djikanović, D., Radotić, K., & Jeremić, M. (2007). Application of asymmetric model in analysis of fluorescence spectra of biologically important molecules. Journal of fluorescence, 17(3), 319-329.

[23] Hunger, K. (Ed.). (2007). Industrial dyes: chemistry, properties, applications. John Wiley & Sons.

[24] Zollinger, H. (2003). Color chemistry: syntheses, properties, and applications of organic dyes and pigments. John Wiley & Sons.

[25] Kasture, P. P., Sonawane, Y. A., Rajule, R. N., & Shankarling, G. S. (2010). Synthesis and characterisation of benzothiazole-based solid-state fluorescent azo dyes. Coloration Technology, 126(6), 348-352.

[26] Ncube, P., Krause, R. W., & Mamba, B. B. (2011). Fluorescent sensing of chlorophenols in water using an azo dye modified β-cyclodextrin polymer. Sensors, 11(5), 4598-4608.

[27] Wolfbeis, O. S. (2005). Materials for fluorescence-based optical chemical sensors. Journal of Materials Chemistry, 15(27-28), 2657-2669.

[28] Lee, L. G., Taing, M. C., & Rosenblum, B. B. (2006). U.S. Patent No. 7,038,063. Washington, DC: U.S. Patent and Trademark Office.

[29] Chen, C. H., Liao, D. J., Wan, C. F., & Wu, A. T. (2013). A turn-on and reversible Schiff base fluorescence sensor for Al 3+ ion. Analyst, 138(9), 2527-2530.

[30] Hsieh, W. H., Wan, C. F., Liao, D. J., & Wu, A. T. (2012). A turn-on Schiff base fluorescence sensor for zinc ion. Tetrahedron letters, 53(44), 5848-5851.

[31] Guo, L., Wu, S., Zeng, F., & Zhao, J. (2006). Synthesis and fluorescence property of terbium complex with novel schiff-base macromolecular ligand. European polymer journal, 42(7), 1670-1675.

[32] Kohn, W., & Sham, L.J. (1965). Self-consistent equations including exchange and correlation effects. Physical Review. 140 (4A), 1133-1138.

[33] Hohenberg, P., & Kohn, W. (1964). Inhomogeneous Electron Gas, Physical Review. 136(3B), 864-871.

[34] Frisch, M., Trucks, G., & Schlegel, H. (2009). G.S.-G. 09, Gaussian, Inc., Wallingford CT.

[35] Bader, R. F. (1991). A quantum theory of molecular structure and its applications. Chemical Reviews, 91(5), 893-928.

[36] Bader, R. F. (1985). Atoms in molecules. Accounts of Chemical Research, 18(1), 9-15.

[37] Lu, T., & Chen, F. (2012). Multiwfn: A multifunctional wavefunction analyzer. Journal of computational chemistry, 33(5), 580-592.

[38] Aydogdu, S., & Hatipoglu, A. (2022). The reaction mechanism investigation of sulfonamides with OH radical by DFT. Journal of the Indian Chemical Society, 99(11), 100752.

[39] Domingo, L. R., & Pérez, P. (2011). The nucleophilicity N index in organic chemistry. Organic & biomolecular chemistry, 9(20), 7168-7175.

SUPPLEMENTARY

Table S1. Calculated electronic parameters of the compounds

Comp.	E (au)	E_{HOMO} (eV)	E_{LUMO} (eV)	ΔE (eV)	η (eV)	χ (eV)	ω (eV)	ε (eV)	α (au)	μ Debye	ω^- (eV)
2a	-1624.80	-6.376	-3.487	2.889	1.445	4.932	8.418	3.119	405.731	6.881	7.036
2a-T	-1624.75	-6.563	-3.213	3.350	1.675	4.888	7.132	2.932	349.324	6.231	6.429
2b	-1533.49	-5.935	-3.069	2.866	1.433	4.502	7.072	3.560	412.928	2.696	6.145
2c	-1644.64	-6.233	-2.943	3.290	1.645	4.588	6.398	3.262	368.272	2.133	5.904
2d	-1413.07	-6.570	-2.932	3.638	1.819	4.751	6.205	2.925	275.568	5.383	5.933
2d-T	-1413.08	-6.093	-2.721	3.372	1.686	4.407	5.760	3.402	302.219	3.350	5.505
2e	-1644.18	-6.185	-2.967	3.218	1.609	4.576	6.507	3.310	362.967	5.790	5.944
2e-T	-1644.20	-6.039	-2.745	3.294	1.647	4.392	5.856	3.456	406.876	2.915	7.036
3a	-1403.10	-5.917	-2.286	3.631	1.816	4.102	4.633	3.578	332.186	0.708	4.821
3b	-1363.79	-5.977	-2.336	3.641	1.821	4.157	4.745	3.518	313.569	1.221	4.906
3c	-1748.16	-6.185	-2.650	3.535	1.768	4.418	5.520	3.310	326.180	3.835	5.411
3d	-1493.11	-6.431	-3.436	2.995	1.498	4.934	8.127	3.064	340.767	8.400	6.904
3e	-1387.81	-6.160	-2.548	3.612	1.806	4.354	5.248	3.335	302.389	3.546	5.253

E: Energy, ΔE: $E_{LUMO} - E_{HOMO}$, η: Chemical Hardness, χ: Electronegativity, ω: Electrophilic index, ε: Nucleophilic index, α: Polarizability, μ: Dipole moment, ω^-: Electrodonating power.
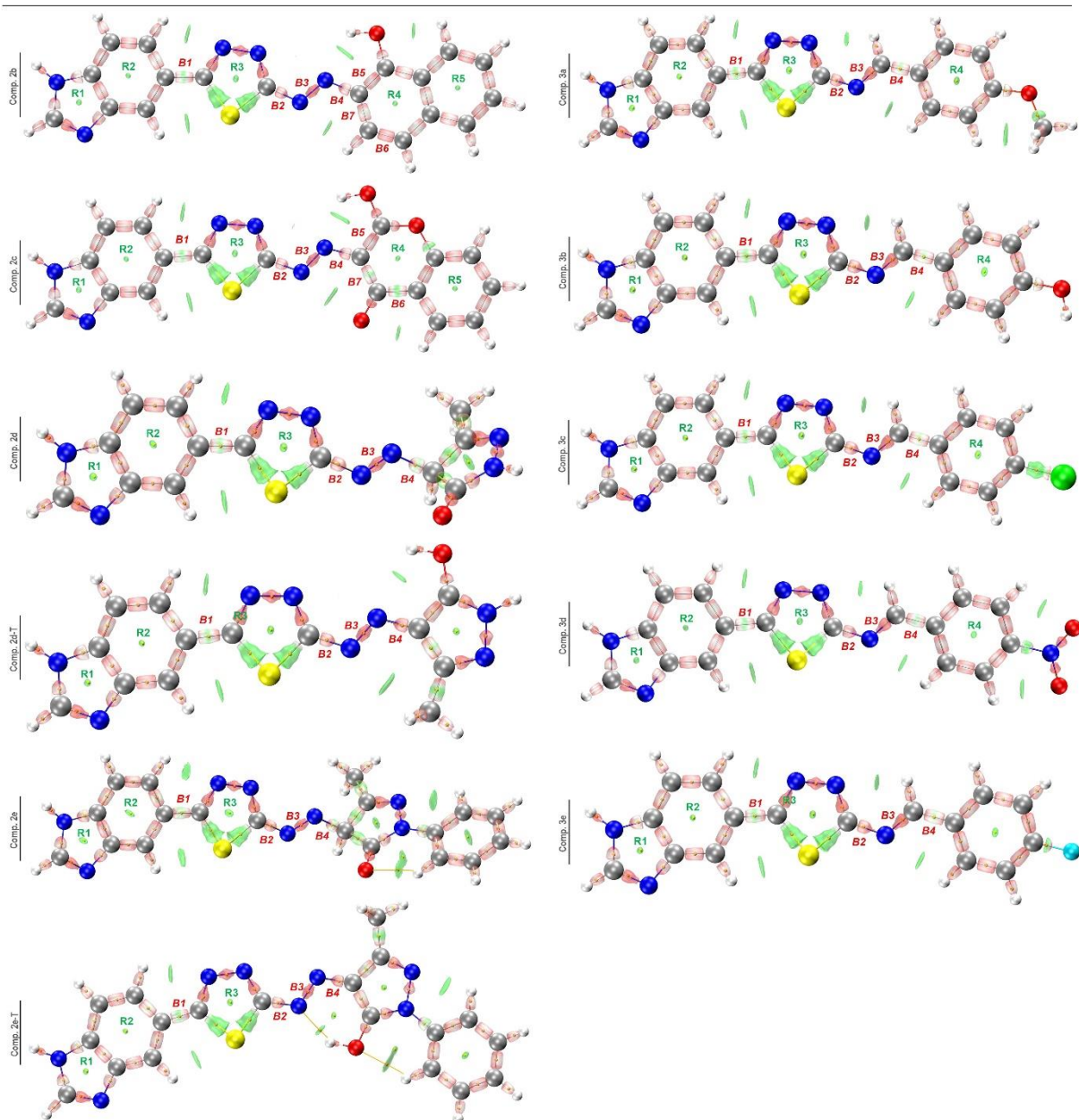
Figure S1. IRI maps of the compounds.